ARTICLE

# Quantum Spin Transport in Carbon Chains

**Zeila Zanolli,[†,‡,⊥,*] Giovanni Onida,[‡,§] and J.-C. Charlier[†,‡]**

[†]Institute of Condensed Matter and Nanosciences (IMCN), Université catholique de Louvain, Place Croix du Sud 1, B-1348 Louvain-la-Neuve, Belgium, [‡]European Theoretical Spectroscopy Facility, Place Croix du Sud 1, B-1348 Louvain-la-Neuve, Belgium, and [§]Dipartimento di Fisica, Università degli Studi di Milano, via Celoria 16, I-20133 Milano, Italy. [⊥]Current address: University of Liege, B-4000 Sart Tilman, Liege, Belgium.

**ABSTRACT** First-principles and non-equilibrium Green's function approaches are used to predict spin-polarized electronic transport in monatomic carbon chains covalently connected to graphene nanoribbons, as recently synthetized experimentally (Jin, C.; *et al. Phys. Rev. Lett.* 2009, *102*, 205501—205504). Quantum electron conductances exhibit narrow resonant states resulting from the simultaneous presence of open conductance channels in the contact region and on the chain atoms. Odd-numbered chains, which acquire metallic or semiconducting character depending on the nature of the edge at the graphene contact, always display a net spin polarization. The combination of electrical and magnetic properties of chains and contacts results in nanodevices with intriguing spintronic properties such as the coexistence of magnetic and semiconducting behaviors.

**KEYWORDS:** linear carbon chain · graphene nanoribbons · quantum electron transport · tunable magnetic properties · tunable electronic properties · *ab initio*

Carbon is a versatile chemical element due to the three possible hybridization states ($sp^3$, $sp^2$, sp) of its atomic orbitals, which correspond to three different prototypical structures: diamond, graphene-like structures (graphite, graphene nanoribbons, carbon nanotubes, fullerenes), and linear carbon chains (known in the literature as carbynes[1]), respectively. Carbynes are traditionally classified as cumulene (monatomic chains with double bonds, ═C═C═) or polyyne (dimerized chains with alternating single and triple bonds, −C≡C−).

While $sp^2$ and $sp^3$ C-based structures have been widely characterized, the synthesis of carbynes has been a challenge for decades due to the high reactivity of chain ends and to a strong tendency for interchain cross-linking.[1] Linear carbon chains consisting of a few tens of atoms were first synthetized *via* chemical methods[2] by stabilizing the chain ends with nonreactive terminal groups.[3−5] However, these systems consist of a mixture of carbon and other chemical elements, and the synthesis of carbynes in a pure carbon environement has only been recently achieved *via* supersonic cluster beam deposition[6,7] and *via* electronic irradiation of graphene inside a transmission electron microscope.[8−10]

In fact, the connections between the carbon chain and the graphitic nanofragments *via* covalent $sp^2$ or $sp^3$ bonds have the twofold effect of stabilizing the chain[11] and providing contacts for charge transport along the chain, suggesting a possible use in nanoelectronics. In addition, the monatomic C chain can be considered as the smallest possible interconnect in all-carbon nanodevices.[12] In particular, the formation of atomic C chains has been suggested to explain the behavior of graphene-based switches,[13] bistable graphitic memories,[14] carbon nanotubes with a "core" thinned down to atomic dimensions,[15,16] and as connections in double-walled nanotubes.[17,18]

To validate the possible exploitation of monatomic C chains as interconnects in pure-C-based electronic devices, it is crucial to investigate the transport properties of such nanostructures connected by graphene-like contacts. Several works have already addressed the problem of the transport properties of carbynes contacted by metallic leads[19−22] and ideal linear C chain leads.[23] However, the properties of a carbon chain connected to graphene-like contacts are expected to be quite different from the latter cases, due to the peculiar linear energy dependence of the conductance in graphene.[24]

## RESULTS AND DISCUSSION

In this work, the study of the spin-polarized electronic transport properties of sp monatomic carbon chains connected to graphene nanoribbons ($C_n$-GNR) is pre-

*Address correspondence to zeilazanolli@gmail.com.

Received for review April 7, 2010 and accepted August 11, 2010.

**Published online August 25, 2010.** 10.1021/nn100712q

sented. Ground-state calculations are performed within the *ab initio* density functional theory (DFT) formalism,[25] and quantum transport is modeled within the non-equilibrium Green's function (NEGF) approach using the one-particle DFT Hamiltonian.[26] Within this formalism, a net spin polarization localized on the chain appears on wires containing an odd number of carbon atoms. In addition, the conductance of the $C_n$-GNR systems is found to be dependent not only on the chain parity but also on the geometrical shape and localization of the $\pi$ states of the chain. Such a behavior could be suggested as the physical mechanism underlying the observed on/off switching of graphene nanodevices.[13] Further, the magnetic and electronic properties of the complex $C_n$-GNR system can be tuned by tailoring the shape of graphene edges (armchair or zigzag) and chain parity to achieve several combinations of spin polarization and electrical conductivity as semiconducting non-spin-polarized, metallic spin-polarized, and even semiconducting spin-polarized structures.

The atomic system under investigation consists of a chain of an even ($C_8$) or odd ($C_9$) number of carbon atoms,[37] contacted by either armchair (AGNR) or zigzag (ZGNR) semi-infinite graphene nanoribbons with hydrogen-saturated edges. The chain is connected to the zigzag profile of the cut AGNR and to the armchair profile of the cut ZGNR with an angle of 120° with respect to the GNR cut edge since GNR atoms have $sp^2$ hybridization, as illustrated in Figure 1 for ZGNR contacts. Graphene nanoribbons (GNRs) are semiconductors with a gap inversely proportional to the ribbon width.[27,28] Hence, to prevent the conductance of the whole system to be limited by the electronic band gap of the GNRs, wide ribbons have been chosen to contact the chain, such as a 35-AGNR (~50 meV band gap) and a 12-ZGNR in both magnetic configurations. Indeed, the zigzag ribbon has been investigated using a ferromagnetic (12-ZGNR-↑ ↑) and an antiferromagnetic (12-ZGNR-↑ ↓) coupling between opposite edges, leading respectively to a metallic or a semiconducting (~280 meV band gap) behavior in agreement with previous *ab initio* calculations.[27]

Transport calculations are performed on atomic systems divided into three regions, as schematically shown in Figure 1: two semi-infinite contacts (left and right leads) and a central scattering region which, in turn, consists of a *core* region embedded by several buffer lead layers. The buffer lead layers are constructed long enough to ensure a good screening of the Hartree potential of the core region in the transport direction (*z*). Convergence studies indicate that the length along the transport direction of the GNR included in the core region has to be 2 times the unit cell for the 35-AGNR and 4 times the unit cell for the 12-ZGNR, leading to a total length of the core region between ~27.5 and ~30 Å.

**Structural and Electronic Properties.** After structural relaxation (for details, please see the Methods section) of

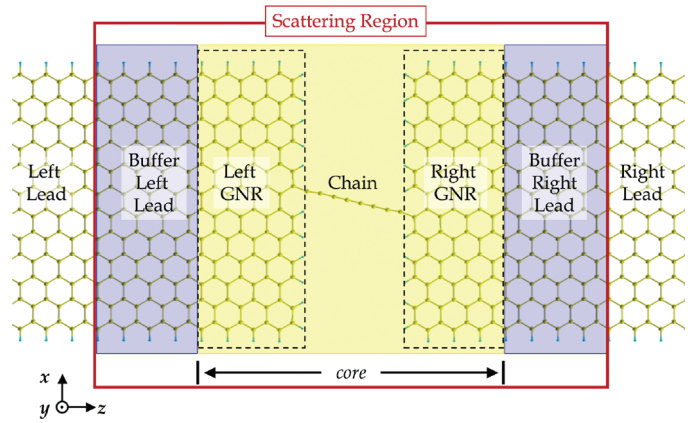


**Figure 1. Schematic representation of the atomic model used to predict transport properties in the case of the $C_8$ chain contacted by ZGNR leads in the transport direction (*z*). The scattering region contains 424 + *n* and 624 + *n* atoms for the $C_n$ chain contacted by 12-ZGNR and 35-AGNR, respectively.**

the core region, the chain binds covalently to a C atom of the contact GNR *via* an $sp^2$ bond. The $C_8$-GNR systems are more stable than the $C_9$-GNR ones with differences in formation energy of 0.787 eV for the 12-ZGNR-↑ ↑ contacts and 0.485 eV for the 35-AGNR contacts, respectively. Ground-state calculations with parallel and antiparallel relative initial spin configuration of the two contact AGNRs have been performed for both $C_8$ and $C_9$ chains. However, after structural relaxation, the magnetization on the zigzag edges of the two AGNRs are always parallel, regardless of the initial assumption. Hence, in what follows, only the case of AGNR contacts with relative parallel orientations will be considered. The systems consisting of chains connected to 12-ZGNR-↑ ↓ exhibit lower total energies (77 and 67 meV for $C_8$ and $C_9$, respectively) than the corresponding structures with ferromagnetic coupling between edges. Since the spin polarization of the ZGNR edges does not affect the structural properties of the chain, only the 12-ZGNR-↑ ↑ case is discussed in this section. The C−C bond lengths in the chain strongly depend on the even or odd parity of the chain. On one hand, the even $C_8$ chains present a larger bond length alternation (BLA) (Figure 2a,c) and hence can be considered as polyyne-like. On the other hand, the odd $C_9$ chains are characterized by a frustrated bond length alternation, leading to an alternation of bond lengths only near the end atoms and bonds of equal length (~1.30 Å) in the middle of the chain (Figure 2b,d). Odd chains have hence a smaller BLA and acquire a cumulene-like character.

The semiconducting or metallic character of the GNR-contacted chains can be directly determined by the relaxed geometry of the chain. Indeed, the electrical properties of ideal 1D monatomic C chains have already been suggested to be directly linked to their $\pi$ states: the $\pi$ orbitals of cumulene being centered on the atoms lead to a metallic system, while the $\pi$ states of polyyne being localized on the triple C≡C bonds in-

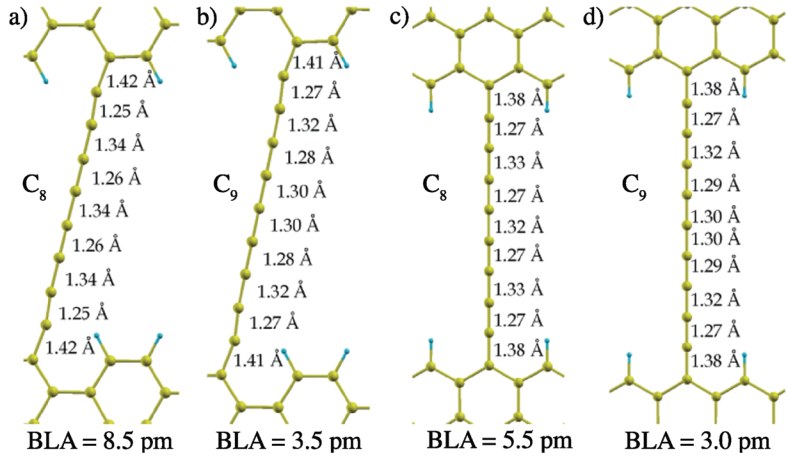


**Figure 2. Relaxed atomic structures, bond lengths, and bond lengths alternation (BLA, in picometers) of the $C_8$ and $C_9$ chains contacted to a 12-ZGNR-↑↑ (a,b) and to a 35-AGNR (c,d), respectively.**

duce a semiconducting behavior.[29] Accordingly, in our $C_n$-GNR systems, we notice that the localization of $\pi$ state wave functions differs for metallic and semiconducting chains: the $\pi$ orbitals of the $C_8$ chain (semiconducting) are localized on the C≡C bonds (Figure 3a,c), while those of the $C_9$-ZGNR-↑↑ chain (metallic) are centered on individual chain atoms (Figure 3b). This picture appears to be consistent with the outcome of Calzolari *et al.*,[29] although a direct comparison cannot be done since the latter uses localized Wannier functions and refers to infinite polyynes and cumulenes. Interestingly, the $C_9$-AGNR case is intermediate because its $\pi$ orbitals are localized on the central C atom and in the middle of the two outermost C≡C bonds (Figure 3d), leading to a semiconducting behavior.

**Magnetic Properties.** Besides their nontrivial electronic properties, the considered sp−$sp^2$ carbon systems are found to display an interesting *magnetic* behavior. To compute the spin density, we use the same nonperiodic open-system scheme as for transport calculations (Figure 1), in order to avoid any unphysical interaction between periodic replicas of the $C_n$-GNR system.[30] Within this formalism, the magnetization of the GNR-contacted chain is predicted to reside mainly on the zigzag edges, as represented in Figure 4, in agreement with the predicted magnetism of zigzag edges in GNRs.[31] However, the presence of a net spin density localized on the chain atoms depends exclusively on the parity of the chain. Indeed, the magnetization on even chains is negligible, while a net spin density is observed on odd chains, as illustrated in Figure 4 and reported in Table 1. In addition, our calculations suggest that the magnetization on the chain is independent of both the magnetic ordering of the GNR edges (ferromagnetic as in 12-ZGNR-↑↑, antiferromagnetic as in 12-ZGNR-↑↓, or spin unpolarized as in 35-AGNR) and on the presence (35-AGNR) or absence (12-ZGNR-↑↑ and 12-ZGNR-↑↓) of magnetization on the contact sides. The same dependence of magnetization on chain parity has also been reported by Ravagnan *et al.*[11] for $C_n$ chains with *n* from 4 to 12 with different kinds of terminations, as H, $H_2$, $C_{20}$, and AGNR. The spin polarization of linear carbon chains is thus an intrinsic property of the chain itself, only depending on the geometrical arrangement of the chain atoms after relaxation and on the resulting presence of unsaturated carbon bonds, since the latter is responsible for magnetism in all-carbon nanostructures.[30] For instance, all four valence electrons of the carbon atoms are employed in forming double bonds in cumulene, while polyyne and even chains can accommodate the exact alternation of single and triple bonds. Hence, in infinite ideal chains and in even chains, all carbon atoms exhibit saturated bonds and no magnetism is expected. On the contrary, odd chains contain an even number of C−C bonds and, hence, the exact alternation of single and triple bonds cannot be achieved. As a consequence, the bond type switches from single/triple (at the chain ends) to double/double (in the middle of the chain), resulting in some uncompensated charge delocalized on the chain and, hence, in a net magnetic moment.

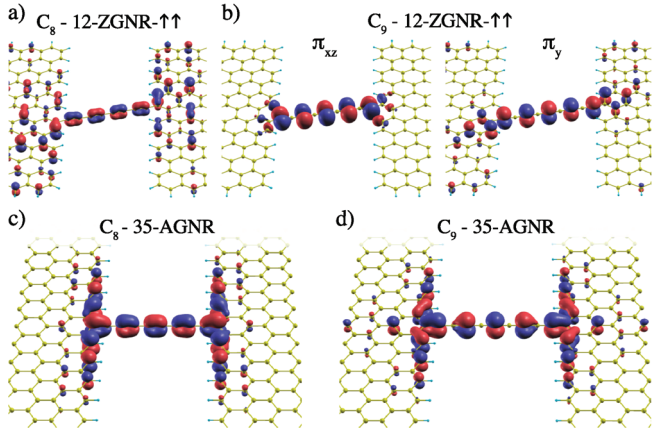


**Figure 3. Wave functions of the $C_n$-GNR systems corresponding to the $\pi$ states on the chain. Blue and red colors correspond to opposite-sign isosurfaces.**

**Quantum Electron Transport.** After the electronic and magnetic properties of the $C_n$-GNR systems were clarified, the investigation of the spin-polarized electron

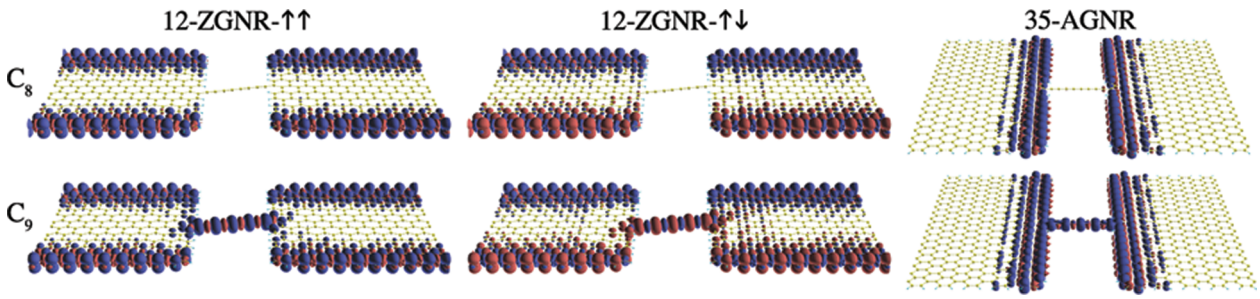


**Figure 4. Spin densities ($\rho_\uparrow - \rho_\downarrow$) on the $C_n$-GNR systems. The $C_8$ (top) and $C_9$ (bottom) chains with the 12-ZGNR-↑↑ (left), 12-ZGNR-↑↓ (middle), and the 35-AGNR (right) contacts are shown. Blue and red correspond to positive and negative isodensities of $\rho_\uparrow - \rho_\downarrow$.**

conductance was then addressed within the NEGF formalism. The latter formalism, in the absence of an external potential and considering a strong coupling between the scattering region and the leads, reduces to the Landauer−Büttiker description for equilibrium transport,[32] where the electron conductance $G(E)$ and the transmission function $T(E)$ at a given energy $E$ are related by $G(E) = T(E)G_0$, where $G_0 = e^2/h$ is the quantum of conductance per spin channel. Within such an approach, the ballistic conductance of ideal GNRs is proportional to the number of conducting channels, that is, the number of bands, at a given energy $E$, resulting in a transmission function with a staircase shape whose height is minimum at the Fermi energy ($E_F$) and increases with energy, as shown by dashed lines in Figure 5 and Figure 6. More specifically, the 12-ZGNR-↑↑ leads are spin-polarized and, hence, their conductance is characterized by two spin channels of $1G_0$ each close to $E_F$. Since both 35-AGNR and 12-ZGNR-↑↓ are small gap semiconductors, their corresponding conductances reduce to zero at $E_F$. The electronic band structure of the ideal infinite carbon chain is not spin-polarized, and it is characterized by a $\sigma$ band, composed by 2s and $2p_z$ atomic orbitals ($z$ being the chain axis) below $E_F$ and by a doubly degenerate $\pi$ band formed by the bonding combinations of the $2p_x$ and $2p_y$ atomic orbitals, which crosses $E_F$ (not shown here). Consequently, the maximal conductance of the ideal chain with ideal contacts amounts to $2G_0$.[23]

The conductance of GNR-contacted chains exhibit, instead, several sharp peaks whose height reaches at most $1G_0$, the conductance per each spin channel of the ideal chain, as illustrated in Figure 5a and Figure 6a,b. To identify the origin of these peaks, the density of states (DOS) has been computed from the Green's function of each open system,[33] in the same energy window as the transmission function $T(E)$. The DOS has been computed for the full scattering region, that is, including both the leads and the chain, as shown in Figure 1, then projected (PDOS) on the $\pi$ orbitals of either the chain or the *left* and *right* GNRs, and finally compared to the respective transmission curves, as illustrated in Figure 5a−c for the structures with 35-AGNR contacts.

In all cases, our calculations predict that the peaks in the transmission function are due to the simultaneous presence of open conductance channels in the contact region and on the chain atoms. The width and the energy position of the resonances depend on the parity of the chain and on the details of the coupling between chain and contact GNRs. Further, it can be noticed that the main features of the conductance of chains connected with 12-ZGNR-↑↑ and 12-ZGNR-↑↓ are unaffected by the magnetic ordering of the GNR edges, apart from the energy band gap of the latter.

The transmission functions of Figure 5 and Figure 6 contain also information on the electrical and magnetic properties of the $C_n$-GNR systems. For instance, even carbon chains behave as semiconductors with a ~1.0 eV gap (Figure 5 and Figure 6, left), consistently with the semiconducting nature of polyynes, regardless of the contact GNRs. Since the $C_8$ chain is not magnetic, the $C_8$-GNR structures inherit the magnetism of the contact GNR, resulting in a magnetic semiconductor whenever the GNR is spin-polarized. Odd chains (Figure 5 and Figure 6, right), being cumulene-like, can lead to metallic $C_n$-GNR structures, and this is, indeed, the case when metallic 12-ZGNR-↑↑ contacts are used. The 12-ZGNR-↑↓ gap, instead, can be identified in the conductance of the $C_9$-12-ZGNR-↑↓ system. Besides, the conductance of the $C_9$ contacted by 35-AGNR reveals a gap of ~1.0 eV per spin channel since this system is semiconducting (Figure 3). On the other hand, given that the $C_9$ is always magnetic, all of the $C_9$-GNR structures, whether they are metallic or semiconducting, are spin-polarized. Hence, magnetism and electrical conductivity of the complex $C_n$-GNR structures are due to the combined properties of both chain and contacts and can, in principle, be tuned to attain semiconducting non-spin-polarized ($C_8$-12-ZGNR-↑↓), metallic spin-polarized ($C_9$-12-ZGNR-↑↑), and even

**TABLE 1. Magnetic Moment ($\mu_B$) on the $C_n$ Chains and on the Total $C_n$-GNR System**

| | $M_{chain}$ ($\mu_B$) | $M_{total}$ ($\mu_B$) |
|---|---|---|
| $C_8$-12-ZGNR-↑↑ | 0.002 | 8.045 |
| $C_8$-12-ZGNR-↑↓ | −0.001 | −0.009 |
| $C_8$-35-AGNR | −0.036 | 7.834 |
| $C_9$-12-ZGNR-↑↑ | 1.405 | 9.672 |
| $C_9$-12-ZGNR-↑↓ | −1.478 | −1.851 |
| $C_9$-35-AGNR | 1.083 | 9.574 |

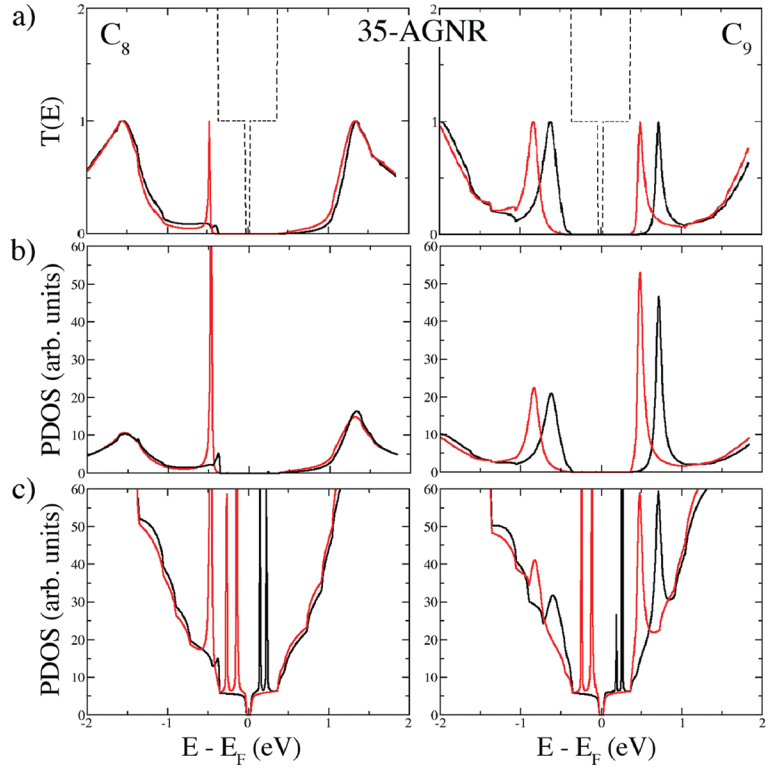


**Figure 5. Solid lines: conductance in units of $G_0$ of the $C_8$ (left panel) and $C_9$ (right panel) chains contacted by AGNR leads (a); PDOS of the $C_n$-35-AGNR systems projected on the $\pi$ states of the chain (b) and of the left contact GNR (c). Dashed lines: conductance of the pristine AGNR leads. Red and black curves are the majority and minority spin channels.**

semiconducting spin-polarized ($C_9$-35-AGNR, $C_8$-35-AGNR, $C_8$-12-ZGNR-$\uparrow\uparrow$, $C_9$-12-ZGNR-$\uparrow\downarrow$) systems.

At last, it can be noticed that the only conducting system, among the investigated structures, is the $C_9$ chain contacted by the 12-ZGNR-$\uparrow\uparrow$. Hence, the reported on/off switching of graphene nanodevices[13] can be due not only to the formation/breaking of a carbon chain between the graphene contacts but also to the parity of the chain and to the geometrical shape and localization of the $\pi$ states of the chain.

## CONCLUSIONS

In conclusion, the magnetic and spin transport properties of linear carbon chains connected with wide GNRs have been investigated from first-principles, using NEGF methods on a set of representative, well-converged prototypical systems. Theoretical results are used for the interpretation of electrical conductivity of such $C_n$-GNR systems, singling out the role of the chain parity and that of the shape and position of the $\pi$ states of the chain. Besides, a net magnetic moment has been

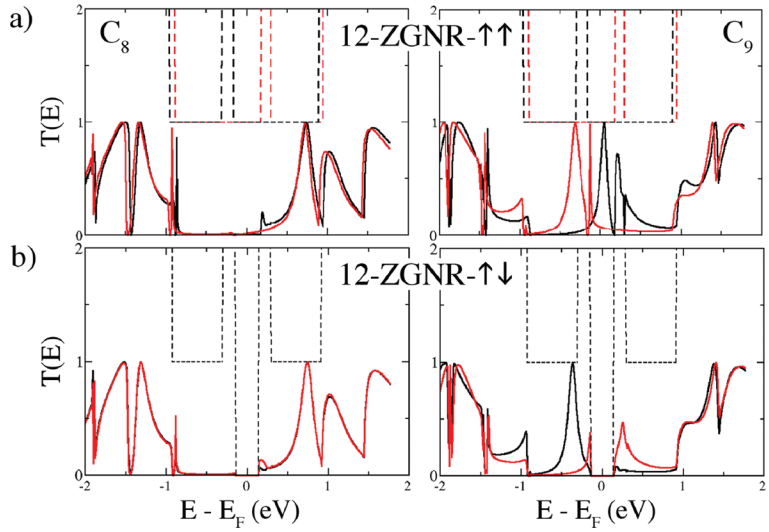


**Figure 6. Solid lines: conductance in units of $G_0$ of the $C_8$ (left panel) and $C_9$ (right panel) chains contacted by ZGNR leads (a,b). Dashed lines: conductance of the pristine ZGNR leads. Red and black curves are the majority and minority spin channels.**

found to be always localized on odd chains and never on even chains, regardless of the magnetic state of the GNR contacts. Finally, the transmission curves show that most of the studied $C_n$-GNR systems behave as spin-polarized semiconductors. Such systems would hence show an intriguing combination of magnetic and transport properties, a clearly interesting feature for potential applications in spintronic devices.

## METHODS

Ground-state calculations are performed within the local spin density approximation (LSDA), using norm-conserving pseudopotentials[34] and numerical atomic orbital basis sets of double-ζ quality (DZ). Due to the good performance of LSDA for carbon-based nanostructures[35] and to the large number of atoms contained in our modeled systems, the latter functional has been preferred over more sophisticated ones (*e.g.*, hybrid functionals). The real-space grid cutoff is 400 Ry; the *k*-point sampling mesh is $1 \times 1 \times 6$, and a Fermi−Dirac distribution function with an electronic temperature of 10 meV is used to populate the energy levels. Basis set quality, *k*-point sampling, kinetic energy cutoff, and electronic temperature have been chosen after accurate convergence studies on the structural, electronic, magnetic, and quantum transport properties of the $G_n$-GNR chain systems. The geometry is fully relaxed until the maximum force on each atom is less than 0.01 eV/Å, and the maximum stress along the *z* direction of the unit cell (*i.e.*, transport direction) is smaller than 0.03 eV/Å. In order to avoid spurious interactions between the periodic replicas of the $G_n$-GNR chain images, the other two dimensions of the cell are kept fixed to guarantee a separation larger than 20 Å between the GNRs' edges and 24 Å between planes.

The computational details for magnetic and transport properties are the same as for ground-state calculation with the exception of the real-space grid cutoff that is 600 Ry (instead of 400 Ry).

The formation energies of the $C_n$-GNR systems ($E_{form}$) are computed as the difference among the total energy of the relaxed $C_n$-GNR structure ($E_{tot}$), the total energy of the GNR ($E_{GNR}$), and *n* times the total energy per atom of the infinite chain ($E_{tot,C}(C_n)$):

$$E_{form} = E_{tot} - E_{GNR} - nE_{tot,C}(C_n)$$

The bond length alternation (or BLA) indicates the degree of dimerization of the chain. Excluding the terminal bonds, it is defined as

$$\frac{1}{2}\left[\sum_{j=1}^{n_e}(d_{2j-1} + d_{n-(2j-1)})/n_e - \sum_{j=1}^{n_0}(d_{2j} + d_{n-2j})/n_0\right]$$

where $d_i = |\vec{r}_i - \vec{r}_{i+1}|$, $n_e = (n + 2)/4$, and $n_0 = n/4$ (integer part).

*Note added in proof:* During the publication process of the present article, we became aware of the recently published work by Zeng *et al.*[36] on the transport properties of $C_7$ and $C_8$ carbon chains contacted by metallic 4-ZGNR, *i.e.*, 4-ZGNR-↑↑.

*Acknowledgment.* J.-C.C. acknowledges financial support from the F.R.S.-FNRS of Belgium. Parts of this work are directly connected to the Belgian Program on Interuniversity Attraction Poles (PAI6) on "Quantum Effects in Clusters and Nanowires", to the ARC on "Hybrid metal/organic nanosystems" sponsored by the Communauté Française de Belgique, and to the European Union through the ETSF e-I3 project (Grant No. 211956). Computational resources have been provided by the Université catholique de Louvain: all the numerical simulations have been performed on the LEMAITRE and GREEN computers of the CISM.

## REFERENCES AND NOTES

1. *Carbyne and Carbynoid Structures*; Heimann, R. B., Evsyukov, S. E., Kavan, L., Eds.; Kluwer Academic: Dordrecht, The Netherlands, 1999.
2. *Polyynes: Synthesis, Properties, and Applications*; Cataldo, F., Ed.; Taylor & Francis: London, 2005.
3. Kavan, L.; Kastner, J. Carbyne Forms of Carbon: Continuation of the Story. *Carbon* **1994**, *32*, 1533–1536.
4. Lagow, R. J.; Kampa, J. J.; Wei, H.-C.; Battle, S. L.; Genge, J. W.; Laude, D. A.; Harper, C. J.; Bau, R.; Stevens, R. C.; Haw, J. F.; Munson, E. Synthesis of Linear Acetylenic Carbon: The "sp" Carbon Allotrope. *Science* **1995**, *267*, 362–367.
5. Eisler, S.; Slepkov, A. D.; Elliott, E.; Luu, T.; McDonald, R.; Hegmann, F. A.; Tykwinski, R. R. Polyynes as a Model for Carbyne: Synthesis, Physical Properties, and Nonlinear Optical Response. *J. Am. Chem. Soc.* **2005**, *127*, 2666–2676.
6. Ravagnan, L.; Siviero, F.; Lenardi, C.; Piseri, P.; Barborini, E.; Milani, P.; Casari, C. S.; Li Bassi, A.; Bottani, C. E. Cluster-Beam Deposition and *In Situ* Characterization of Carbyne-Rich Carbon Films. *Phys. Rev. Lett.* **2002**, *89*, 285506–285509.
7. Ravagnan, L.; Piseri, P.; Bruzzi, M.; Miglio, S.; Bongiorno, G.; Baserga, A.; Casari, C. S.; Li Bassi, A.; Lenardi, C.; Yamaguchi, Y.; Wakabayashi, T.; Bottani, C. E.; Milani, P. Influence of Cumulenic Chains on the Vibrational and Electronic Properties of $sp-sp^2$ Amorphous Carbon. *Phys. Rev. Lett.* **2007**, *98*, 216103–216106.
8. Meyer, J. C.; Girit, C. O.; Crommie, M. F.; Zettl, A. Imaging and Dynamics of Light Atoms and Molecules on Graphene. *Nature* **2008**, *454*, 319–322.
9. Jin, C.; Lan, H.; Peng, L.; Suenaga, K.; Iijima, S. Deriving Carbon Atomic Chains from Graphene. *Phys. Rev. Lett.* **2009**, *102*, 205501–205504.
10. Chuvilin, A.; Meyer, J. C.; Algara-Siller, G.; Kaiser, U. From Graphene Constrictions to Single Carbon Chains. *New J. Phys.* **2009**, *11*, 083019.
11. Ravagnan, L.; Manini, N.; Cinquanta, E.; Onida, G.; Sangalli, D.; Motta, C.; Devetta, M.; Bordoni, A.; Piseri, P.; Milani, P. Effect of Axial Torsion on sp Carbon Atomic Wires. *Phys. Rev. Lett.* **2009**, *102*, 245502–245505.
12. Avouris, P.; Chen, Z.; Perebeinos, V. Carbon-Based Electronics. *Nat. Nanotechnol.* **2007**, *2*, 605–615.
13. Standley, B.; Bao, W.; Zhang, H.; Bruck, J.; Lau, C. N.; Bockrath, M. Graphene-Based Atomic-Scale Switches. *Nano Lett.* **2008**, *8*, 3345–3349.
14. Li, Y.; Sinitskii, A.; Tour, J. M. Electronic Two-Terminal Bistable Graphitic Memories. *Nat. Mater.* **2008**, *7*, 966–971.
15. Yuzvinsky, T. D.; Mickelson, W.; Aloni, S.; Begtrup, G. E.; Kis, A.; Zettl, A. Shrinking a Carbon Nanotube. *Nano Lett.* **2006**, *6*, 2718–2722.
16. Khoo, K. H.; Neaton, J. B.; Son, Y. W.; Cohen, M. L.; Louie, S. G. Negative Differential Resistance in Carbon Atomic Wire-Carbon Nanotube Junctions. *Nano Lett.* **2008**, *8*, 2900–2905.
17. Endo, M.; Muramatsu, H.; Hayashi, T.; Kim, Y.; Van Lier, G.; Charlier, J.; Terrones, H.; Terrones, M.; Dresselhaus, M. Atomic Nanotube Welders: Boron Interstitials Triggering Connections in Double-Walled Carbon Nanotubes. *Nano Lett.* **2005**, *5*, 1099–1105.
18. Fantini, C.; Cruz, E.; Jorio, A.; Terrones, M.; Terrones, H.; Van Lier, G.; Charlier, J.; Dresselhaus, M.; Saito, R.; Kim, Y.; Hayashi, T.; Muramatsu, H.; Endo, M.; Pimenta, M. Resonance Raman Study of Linear Carbon Chains Formed by the Heat Treatment of Double-Wall Carbon Nanotubes. *Phys. Rev. B* **2006**, *73*, 193408.
19. Lang, N.; Avouris, P. Oscillatory Conductance of Carbon-Atom Wires. *Phys. Rev. Lett.* **1998**, *81*, 3515–3518.
20. Lang, N.; Avouris, P. Carbon-Atom Wires: Charge-Transfer Doping, Voltage Drop, and the Effect of Distortions. *Phys. Rev. Lett.* **2000**, *84*, 358–361.

21. Larade, B.; Taylor, J.; Mehrez, H.; Guo, H. Conductance, *I*−*V* Curves, and Negative Differential Resistance of Carbon Atomic Wires. *Phys. Rev. B* **2001**, *64*, 075420.
22. Crljen, Z.; Baranovic, G. Unusual Conductance of Polyyne-Based Molecular Wires. *Phys. Rev. Lett.* **2007**, *98*, 116801–116804.
23. Tongay, S.; Senger, R.; Dag, S.; Ciraci, S. Ab Initio Electron Transport Calculations of Carbon Based String Structures. *Phys. Rev. Lett.* **2004**, *93*, 136404–136407.
24. Chen, W.; Andreev, A. V.; Bertsch, G. F. Conductance of a Single-Atom Carbon Chain with Graphene Leads. *Phys. Rev. B* **2009**, *80*, 085410.
25. Soler, J. M.; Artacho, E.; Gale, J. D.; Garcia, A.; Junquera, J.; Ordejon, P.; Sanchez-Portal, D. The SIESTA Method for *Ab Initio* Order-N Materials Simulation. *J. Phys.: Condens. Matter* **2002**, *14*, 2745–2779.
26. Rocha, A. R.; Garcia-Suarez, V. M.; Bailey, S.; Lambert, C.; Ferrer, J.; Sanvito, S. Spin and Molecular Electronics in Atomically Generated Orbital Landscapes. *Phys. Rev. B* **2006**, *73*, 085414.
27. Son, Y.-W.; Cohen, M. L.; Louie, S. G. Energy Gaps in Graphene Nanoribbons. *Phys. Rev. Lett.* **2006**, *97*, 216803–216806.
28. Dubois, S. M. M.; Zanolli, Z.; Declerck, X.; Charlier, J. C. Electronic Properties and Quantum Transport in Graphene-Based Nanostructures. *Eur. Phys. J. B* **2009**, *72*, 1–24.
29. Calzolari, A.; Marzari, N.; Souza, I.; Nardelli, M. *Ab Initio* Transport Properties of Nanostructures from Maximally Localized Wannier Functions. *Phys. Rev. B* **2004**, *69*, 035108.
30. Zanolli, Z.; Charlier, J. C. Spin Transport in Carbon Nanotubes with Magnetic Vacancy-Defects. *Phys. Rev. B* **2010**, *81*, 165406.
31. Wakabayashi, K.; Fujita, M.; Ajiki, H.; Sigrist, M. Electronic and Magnetic Properties of Nanographite Ribbons. *Phys. Rev. B* **1999**, *59*, 8271–8282.
32. Buttiker, M.; Imry, Y.; Landauer, R.; Pinhas, S. Generalized Many-Channel Conductance Formula with Application to Small Rings. *Phys. Rev. B* **1985**, *31*, 6207–6215.
33. Rocha, A. R.; Padilha, J. E.; Fazzio, A.; da Silva, A. J. R. Transport Properties of Single Vacancies in Nanotubes. *Phys. Rev. B* **2008**, *77*, 153406.
34. Troullier, N.; Martins, J. L. Efficient Pseudopotentials for Plane-Wave Calculations. *Phys. Rev. B* **1991**, *43*, 1993–2006.
35. Charlier, J.-C.; Blase, X.; Roche, S. Electronic and Transport Properties of Nanotubes. *Rev. Mod. Phys.* **2007**, *79*, 677–732.
36. Zeng, M. G.; Shen, L.; Cai, Y. Q.; Sha, Z. D.; Feng, Y. P. Perfect Spin-Filter and Spin-Valve in Carbon Atomic Chains. *Appl. Phys. Lett.* **2010**, *96*, 042104.
37. Since even and odd chains have been found to have different magnetic properties,[11] chains containing 8 and 9 atoms have been chosen to represent the two magnetic behaviors. Very short chains (such as $C_4$ and $C_3$) have not been considered for the present work because, in that case, the quantum conductance is dominated by tunneling through the chain.[16] $C_8$ and $C_9$ have, then, been chosen after taking into account that synthesized carbon chains contain, at most, a few tens of carbon atoms.[2]